Intravenous and oral copper kinetics, biodistribution and dosimetry in healthy humans studied by [^{64}Cu]copper PET/CT

Kristoffer Kjærgaard (krikje@clin.au.dk)
Department of Nuclear Medicine and PET-Centre, Aarhus University Hospital; Department of Hepatology and Gastroenterology, Aarhus University Hospital https://orcid.org/0000-0002-6440-2784

Thomas Sandahl
Department of Hepatology and Gastroenterology, Aarhus University Hospital

Kim Frisch
Department of Nuclear Medicine and PET-Centre, Aarhus University Hospital

Karina Højrup Vase
Department of Nuclear Medicine and PET-Centre, Aarhus University Hospital

Susanne Keiding
Department of Hepatology and Gastroenterology, Aarhus University Hospital; Department of Nuclear Medicine and PET-Centre, Aarhus University Hospital

Hendrik Vilstrup
Department of Hepatology and Gastroenterology, Aarhus University Hospital

Peter Ott
Department of Hepatology and Gastroenterology, Aarhus University Hospital

Lars Christian Gormsen
Department of Nuclear Medicine and PET-Centre, Aarhus University Hospital

Ole Lajord Munk
Department of Nuclear Medicine and PET-Centre, Aarhus University Hospital

Research article

Keywords: 64Cu, copper, kinetics, dosimetry, biodistribution

Posted Date: April 22nd, 2020

DOI: https://doi.org/10.21203/rs.3.rs-23655/v1

Version of Record: A version of this preprint was published at EJNMMI Radiopharmacy and Chemistry on June 18th, 2020. See the published version at https://doi.org/10.1186/s41181-020-00100-1.

Abstract

Purpose: Copper is essential for enzymatic processes throughout the body. [^{64}Cu]copper (^{64}Cu) positron emission tomography (PET) has been investigated as a diagnostic tool for certain malignancies, but has not yet been used to study copper homeostasis in humans. In this study, we determined the hepatic removal kinetics, biodistribution and radiation dosimetry of ^{64}Cu in healthy humans by both intravenous and oral administration of the radiotracer.

Methods: Six healthy participants underwent PET/CT studies with intravenous or oral administration of ^{64}Cu. A 90 min dynamic PET scan of the liver was followed by three whole-body PET/CT scans at 1.5, 6, and 20 h after tracer administration. PET data were used for estimation of hepatic kinetics, biodistribution, effective doses, and absorbed doses for critical organs.

Results: After intravenous administration, ^{64}Cu uptake was highest in the liver, intestinal walls and pancreas; the gender-averaged effective dose was 62 ± 5 μSv/MBq (mean ± SD). After oral administration, ^{64}Cu was almost exclusively taken up by the liver while leaving a significant amount of residual radiotracer in the gastrointestinal lumen, resulting in an effective dose of 113 ± 1 μSv/MBq. Excretion of ^{64}Cu in urine and faeces after intravenous administration was negligible. Hepatic removal kinetics showed that ^{64}Cu clearance from blood was 0.10 ± 0.02 mL blood/min/mL liver tissue, and the rate constant for excretion into bile or blood was 0.003 ± 0.002 min^{-1}.

Conclusion: ^{64}Cu biodistribution and radiation dosimetry are affected by the manner of tracer administration with high uptake by the liver, intestinal walls, and pancreas after intravenous administration; after oral administration, ^{64}Cu is rapidly absorbed from the gastrointestinal tract and deposited primarily in the liver. Administration of 50 MBq ^{64}Cu yielded images of high quality for both administration forms with radiation doses approximately 3.1 and 5.7 mSv, respectively, allowing for sequential studies in humans.

Trial Registration Number: EudraCT no. 2016-001975-59. Registration date: 19/09/2016.

Introduction

Copper is an essential mineral present in all tissues and is important for several enzymatic processes [1]. It is absorbed in the upper intestine and subsequently taken up by the liver via the portal vein. From the liver, copper is either distributed to the systemic circulation bound to ceruloplasmin or, in the case of excess, excreted into the bile [2]. Disturbances in copper homeostasis are potentially fatal as seen in the rare genetic disorder of Wilson's disease, where accumulation of toxic levels of copper in various organs leads to critical symptoms from the liver and central nervous system [3].

Human copper metabolism and kinetics are only partly understood despite recent advances in molecular imaging, notably positron emission tomography (PET). [^{64}Cu]copper (^{64}Cu) PET is characterized by high

spatial and temporal resolution, and the radioactive half-life of ^{64}Cu ($t_{1/2}$ = 12.7 h) allows for *in vivo* assessment of copper biodistribution, even in compartments with slow copper turnover. To date, only few ^{64}Cu PET studies of biodistribution and radiation dosimetry after intravenous injection in humans have been published, but it remains unclear which organs are most critical in terms of radiation exposure [4–6]. In addition, no such studies have been published on oral administration of ^{64}Cu, the natural entrance route of copper in humans.

^{64}Cu PET/CT has been used in the context of cancer detection and characterization [5–8], utilizing the overexpression of the human copper transporter 1 (CTR1) in malignant cells [9]. To our knowledge, no studies have yet examined the potential of ^{64}Cu PET/CT to assess temporal whole-body copper homeostasis in humans, in particular hepatic copper uptake, accumulation and excretion.

In this study, we determined the hepatic kinetics of ^{64}Cu, characterized copper biodistribution and estimated the radiation dosimetry of ^{64}Cu in healthy humans by sequential whole-body PET imaging spanning 1.5 to 20 h after intravenous or oral administration. The image based biodistribution estimates were supplemented by measurements of radioactive concentrations in blood, urine and faecal samples.

Materials And Methods

Radiochemistry

Solid $^{64}CuCl_2$ (radionuclidic purity ≥ 99%; specific activity ≥ 1.0 TBq/µmol) was supplied by the Hevesy Laboratory, DTU Nutech, Risø, Roskilde, Denmark. The received $^{64}CuCl_2$ was dissolved in sterile 0.1 M HCl (1 mL), pH was adjusted to around 5 with sterile 0.5 M sodium acetate buffer (0.5 mL), and sterile saline (8.5 mL) was added. The acetate buffered ^{64}Cu solution was finally passed through a sterilizing filter (0.22 µm) into a sterile product vial. Quality control of the ^{64}Cu solution consisted of pH measurement (pH strips; specification: 4–6), radiochemical purity test (radio-TLC; specification: ≥95%), LAL-test (PTS Endosafe, Charles River Laboratories; specification: <17.5 EU/ml), radionuclide identification (gamma spectrum; germanium detector; specification: 511 + 1346 keV), and sterile filter test (pressure-hold-test; specification: filter intact). The preparation and quality control of the ^{64}Cu solution was approved by the Danish Medicines Agency.

Study Design and Participants

Biodistribution and dosimetry for ^{64}Cu after intravenous and oral administration were determined by dynamic liver and subsequent whole body PET/CT in six healthy human participants (age 22–61 years). Four participants received intravenous administration (IV1-IV4; two males, two females) and two received oral administration (O1-O2; one male, one female) of ^{64}Cu (Table 1). In an additional four participants (IV5-IV8; 2 males, two females) blood, urine, and faecal samples were collected after intravenous ^{64}Cu administration, but without PET imaging (Supplemental Table 1). Participants fasted for at least 6 h

before administration of ^{64}Cu, but were allowed to drink water. Study inclusion criteria were: Age above 18 years, and for females, negative pregnancy test and use of safe contraception. Criteria for exclusion were known hypersensitivity to ingredients in the formula, history of clinical disease, current pregnancy, breastfeeding, or desire to become pregnant. No complications to the procedures were observed.

Table 1
Patient characteristics, gender-averaged absorbed dose estimates (μGy/MBq), and effective dose (μSv/MBq) for ^{64}Cu by intravenous (IV) and oral administration

	IV				**Oral**	
ID (sex/age)	IV1 (M/61)*	IV2 (F/25)	IV3 (M/24)	IV4 (F/22)	O1 (F/39)	O2 (M/27)
BW/height (kg/cm)	76/178	74.7/175	94/186	68/160	54/168	77/181
Dose (MBq)	116.4	66.04	73.0	77.0	57.3	61.3
Target organ						
Liver	415.0	467.0	462.0	446.0	317.0	335.0
Gallbladder	87.8	108.0	126.0	68.4	144.0	119.0
Stomach	48.3	61.1	58.0	48.8	274.0	238.0
Small Intestine	188.0	238.0	191.0	168.0	369.0	395.0
RLI	225.0	88.7	181.0	213.0	925.0	600.0
LLI	250.0	87.1	120.0	121.0	30.4	375.0
Kidneys	137.0	128.0	133.0	132.0	66.0	72.6
Pancreas	116.0	122.0	110.0	173.0	51.8	51.5
Red Bone Marrow	36.2	34.0	35.5	32.5	27.0	24.4
Effective Dose	67.6	56.2	62.0	61.3	114.0	112.0
Data for critical target organs and effective doses for all individuals; for full list of organs, see Supplemental Table 2.						
*Dynamic PET/CT scan and blood samples not obtained.						
BW = Body Weight; RLI = Right Large Intestine; LLI = Left Large Intestine.						

PET/CT Acquisition

The participants were placed in supine position in a Siemens Biograph™ 64 TruePoint™ PET/CT camera within the 21.6 cm axial field-of-view. A low dose CT scan (50 effective mAs with CARE Dose4D, 120 kV, pitch of 0.8 mm, slice thickness 5.0 mm) was performed before each PET scan for definition of anatomic

structures and attenuation correction of the PET images. The ^{64}Cu solution was administered as an intravenous bolus injection (n = 4; median dose 73.5 MBq, range 66–116 MBq) or dissolved in water and swallowed (n = 2; median dose 65.5 MBq, range 57–74 MBq). All participants underwent a dynamic PET scan of 90 min (dynamic PET and blood sampling were not acquired for one participant, see Table 1) with field-of-view over the liver, recorded in list-mode; time frame structure was 12 × 5 s, 8 × 15 s, 7 × 60 s, and 16 × 300 s. This was followed by three consecutive whole-body PET/CT scans (top of skull to mid-thigh; 6 bed positions) performed at 1.5, 6, and 20 h after tracer administration (duration 6, 6, and 10 min per bed position). The PET images were reconstructed using 3-dimensional ordered-subset expectation maximization with 4 iterations and 21 subsets, 4-mm Gauss filter, and 168 × 168 matrix with voxel size 4 × 4 × 5mm^3.

Image Processing

The fused PET/CT images were analysed using the PMOD 3.7 software (PMOD Technologies Ltd, Zürich, Switzerland). For kinetic analysis, the time course of the activity concentration of ^{64}Cu during the 90-min dynamic PET scan was measured in a volume-of-interest (VOI) placed in the right liver lobe. The VOIs were drawn to contain liver tissue while avoiding large intrahepatic blood vessels and bile ducts. For biodistribution and dosimetry calculations, all tissues were visually inspected on images of the 1.5 h, 6 h, and 20 h whole body scans by two investigators. Organs with accumulation of ^{64}Cu above that of surrounding tissue were defined as source organs: liver, gallbladder contents, small intestine, left large intestine (descending and sigmoid colon), right large intestine (ascending and transverse colon), rectum, stomach contents, kidneys, pancreas (IV only), and red bone marrow. VOIs were manually drawn for each source organ to encompass all radioactivity of the respective organ. The red bone marrow activity was estimated based on VOIs in the lumbar vertebrae as described by McParland [10].

Blood, Urine and Faecal Samples

In the intravenous study, arterial blood samples were collected from a radial artery during the initial dynamic PET scan at time points 12 × 5 s, 8 × 15 s, 7 × 60 s, and 16 × 300 s. In the oral study, venous blood samples were collected from a peripheral vein during the initial dynamic PET scan and before each of the consecutive whole-body scans (1.5 h, 6 h, and 20 h). In additional four participants with intravenous tracer administration (IV5-8), venous blood samples were obtained as for the oral study, and total urine and faeces were collected from 0–6 h and 6–20 h. Radioactivity concentrations of ^{64}Cu were measured in whole blood, plasma, urine, and faeces using a well gamma counter (Packard 5003, Packard Instruments, USA). Time courses of the activity concentration in blood and plasma were generated for 90 min with two additional samples at 6 h and 20 h. Total output in percent of administered dose (%AD) for urine and faeces were calculated for time points 6 h and 20 h. All concentration measurements were cross-calibrated with the PET-camera and corrected for radioactive decay back to start of the tracer administration.

Modelling of Hepatic Kinetics

Kinetic parameters were estimated by fitting kinetic models to the dynamic liver PET data using the time course of arterial plasma ^{64}Cu as input function. To account for the hepatic dual blood supply from the hepatic artery (25%) and portal vein (75%), we used reversible linearised models that allow robust and unbiased estimates using only the arterial input function [11]. Two kinetic models were used: 1) The Gjedde-Patlak linearisation yielding the steady-state clearance from blood to liver tissue (K; mL blood/min/mL liver tissue) including a small reversible loss rate constant (k_{loss}; min^{-1}), representing the loss of tracer from the liver hepatocytes into bile or blood [12]; 2) the Logan linearisation [13] that estimates the total distribution volume (V_d; mL blood/mL liver tissue) of ^{64}Cu in the liver. Both kinetic models were applied to data 30 to 90 min after tracer administration to ensure quasi-steady-state. The kinetic model parameters were estimated using software developed in-house (http://www.liver.dk/ifit.html; v0.82).

Biodistribution and Dosimetry

For each source organ, the time course of the non-decay-corrected total radioactivity was normalised to the administered activity and recalculated to time courses of percentage injected activity. Time-integrated activity coefficients (TIACs) were computed using the trapezoidal integration method to calculate the area under the curves, assuming only physical decay after the last scan without further biological clearance. The remainder TIAC was calculated by subtracting the individual source organ TIACs from the total body TIAC (without voiding), which for ^{64}Cu is 18.3 h. TIACs for source organs and remainder were used in OLINDA/EXM 2.0 (HERMES Medical Solution AB, Sweden) [14] to compute organ absorbed doses (μGy/MBq) and the effective dose (μSv/MBq) using anthropomorphic human body phantoms with organ masses based on ICRP89 [15] and ICRP103 tissue weighting factors [16]. Organ doses and effective dose results are given for the reference gender-averaged adult according to ICRP103.

Results

Biodistribution

Figures 1 and 2A-B show whole-body PET/CT and time-activity curves for the biodistribution of ^{64}Cu. ^{64}Cu was avidly taken up by the liver after both intravenous and oral administration with the highest concentrations reached after 6 h, where %AD in the liver was 47 ± 1.35% and 34 ± 0.01% (mean ± SD), respectively. In addition, considerable radioactivity was observed in the red bone marrow and kidneys. Uniquely for the intravenous administration, ^{64}Cu was taken up by the pancreas, intestinal walls, and salivary glands (Fig. 1). After oral administration, the biodistribution of ^{64}Cu was dominated by efficient uptake by the liver and varying degrees of residual activity in the intestinal lumen. Approximately 1.5 h after administration for both groups, the variation in biodistribution between the participants was insignificant (Fig. 2A-B). Accumulation of ^{64}Cu in other organs, including the brain, urinary bladder, and prostate was negligible.

The hepatic uptake of ^{64}Cu was rapid after intravenous administration, whereas the uptake following oral administration was delayed (approximately 12 min) by the process of intestinal absorption (Fig. 2C-D). Apart from the delay, the rate of uptake in liver tissue was comparable between the two administration forms with %AD in the liver peaking at 6 h followed by a minor decrease, most likely caused by biliary excretion and redistribution back to blood. The gallbladder was visible on the PET images in five of the six participants after 1.5 h, indicating some degree of biliary excretion at this time.

Hepatic Kinetics

Analysis of the hepatic removal kinetics of ^{64}Cu following intravenous administration provided robust linear model-fits to the liver PET data (examples in Supplemental Fig. 1). The steady-state hepatic clearance of ^{64}Cu from blood into liver tissue (K) was 0.10 ± 0.02 mL blood/min/mL liver tissue with marginal loss of tracer into bile or blood (k_{loss} = 0.003 ± 0.002 min^{-1}); the hepatic volume of distribution (V_d) was 36 ± 22 mL blood/mL liver tissue (mean ± SD; n = 3).

Blood, Urine and Faeces

After intravenous administration, arterial ^{64}Cu was rapidly cleared from the systemic circulation; the whole-blood to plasma activity ratio was approximately 55%, increasing slowly during the initial 90 min (Fig. 3A). The venous ^{64}Cu showed a similar pattern and increased slowly for the remaining study period (Fig. 3B). After oral administration, venous blood concentrations increased until approximately 1 hour and then gradually subsided before a slow increase, comparable to that observed after intravenous administration (Fig. 3B). The low radioactivity concentration in venous blood following oral administration illustrates the efficient first-pass extraction of ^{64}Cu through the liver.

After intravenous administration, insignificant amounts of ^{64}Cu were measured in urine (mean %AD ± SD: 0.0013 ± 0.0006) and faeces (median %AD [range]: 0.0022 [0.0002–0.0416]) during the study period (Supplemental Fig. 2). Urine and faeces were not collected after oral administration.

Radiation Dosimetry

Participant characteristics and dosimetry data are given in Table 1; the full list of organs is given in Table S2. After intravenous administration, the most critical organ was the liver (range 415–467 µGy/MBq), followed by the small intestines (range 168–238 µGy/MBq). After oral administration, the most critical organ was the right large intestine (range 600–925 µGy/MBq), followed by the small intestines (range 369–378 µGy/MBq), liver (range 317–335 µGy/MBq), and stomach (range 238–274 µGy/MBq). Importantly, the radiation exposure to the intestines was highly dependent on individual peristalsis and intestinal transit time as observed in participant O1 where the right large intestine received as much as 925 µGy/MBq and the left large intestine, almost nothing. In contrast, the radiation dose to the liver varied very little between the participants for both administration forms. The gender-averaged effective doses after intravenous and oral administration were 62 ± 5 and 113 ± 2 µSv/MBq (mean ± SD).

Discussion

In this study, we report ^{64}Cu PET/CT results on biodistribution, dosimetry, and hepatic removal kinetics following both intravenous and oral administration of the radiotracer in healthy humans.

^{64}Cu Biodistribution

Following absorption in the intestines, copper is transported into the portal blood circulation by the ATP7A transporter located in the basolateral membrane of the enterocytes [17]. In the portal vein, copper is bound to albumin, in particular, and to other plasma proteins in a highly exchangeable pool [18, 19]. Albumin-bound copper in systemic plasma has a half-life of 10–20 min [20] and is effectively extracted during the hepatic first pass (> 80%) [21]. In the present study, high uptake of ^{64}Cu from the systemic circulation after intravenous administration was also observed in other tissues characterised by high expression of the CTR1 transporter such as the pancreas, intestinal walls, and kidneys [22]. After intravenous administration, ^{64}Cu was not excreted in urine and only a negligible amount was detected in faeces during the 20-hour observation period.

After oral administration, the biodistribution was dominated by efficient hepatic first pass extraction of ^{64}Cu [20], whereas uptake in organs other than the liver, kidneys, and red bone marrow was negligible when compared with intravenous administration. Moreover, the total %AD taken up from the intestines and measured in source organs did not exceed 50%, which is in accordance with net intestinal copper absorption studies in pigs and humans [19, 23]. It should be noted that the intestinal absorption of copper is affected by the dietary composition and our results therefore only reflect conditions in the 6 h fasting state [24].

In the liver, copper is incorporated in ceruloplasmin (biological half-life: 13 hours) and then redistributed into the systemic circulation 2–3 days after administration, creating a second peak in blood concentration, also known as the ceruloplasmin wave [25, 26]. In the present study, the blood concentration of ^{64}Cu steadily increased after the peak following administration, reflecting copper incorporation into ceruloplasmin. The arterial blood to plasma radioactivity ratio was approximately 55% and increased over the first 90 min, possibly reflecting copper uptake in erythrocytes by the anion exchanger located in the erythrocyte membrane [27].

^{64}Cu Dosimetry

Dosimetry estimates for intravenous administration showed that the liver was the most critical organ, followed by the small intestines. Reports of dosimetry estimates for intravenous administration of ^{64}Cu differ to some extent. In the present study, radiation exposure to the liver and intestines was considerably higher and the effective dose twice of what was previously reported in patients with prostate cancer [5, 6]. This difference is likely caused by different analytical approaches rather than altered biodistribution of ^{64}Cu in patients with prostate cancer compared with healthy subjects. However, our results, based on the

newest phantoms and tissue weighing factors [14–16], are in agreement with the observations made by Avila-Rodriguez et al. in healthy participants [4].

To our knowledge, dosimetry estimates for oral administration of ^{64}Cu have not previously been reported. As expected, the radiation dosimetry of ^{64}Cu after oral and intravenous administration differed significantly. While the liver was exposed to a high radiation dose after oral administration, equal or higher doses were received by the intestines due to high amounts of unabsorbed radiotracer. In this context, it is important to acknowledge that the radiation dose to the intestines depends on the individual intestinal transit time, unlike for intravenous administration; in our study, one participant received 925 µGy/MBq to the right large intestine. Consequently, radiation dosimetry of ^{64}Cu by oral administration may differ substantially between individuals necessitating a cautious approach to total oral dose used in future studies. Based on our results, the total radiation dose received by the reference gender-averaged adult after an oral ingestion of 50 MBq ^{64}Cu amounts to 5.6 mSv, ensuring less than 50 mSv absorbed by a single organ. This dose is sufficient to obtain high-quality PET images, and may still be reduced by at least 50% with new digital PET systems yielding faster time-of-flight timing resolution and higher NEMA sensitivity. Thus, ^{64}Cu PET using intravenous or oral administration is suitable for studying copper metabolism in humans.

Copper Metabolism

The use of radioactive Cu isotopes to assess copper metabolism in humans was introduced decades ago and many studies on this topic have been published since then [28–31]. Most recently, Czlonkowska et al. showed that measurements of ^{64}Cu in blood and in urine following intravenous injection accurately distinguished between patients with Wilson's disease and heterozygote controls [31]. The obvious advantage of ^{64}Cu-copper PET/CT is however, the potential for assessing also the hepatic uptake, accumulation, and turnover; this includes oral administration where the biodistribution is dominated by first pass extraction by the liver, as demonstrated in the present study. In addition, the PET/CT data on the accumulation of protein-bound ^{64}Cu reported in this study provides valuable knowledge to help interpret unwanted copper loss in relation to the increasing research on ^{64}Cu radiopharmaceuticals.

Peng et al. assessed hepatic copper kinetics in rats using ^{64}Cu PET/CT [32], revealing some noteworthy differences between rodents and our human participants. For example, cardiac uptake of ^{64}Cu was substantial in rodents whereas it was negligible in our human participants. Results from rodent copper studies can therefore not be easily translated to human conditions. In the present study, we were able to quantify the hepatic removal kinetics of ^{64}Cu using dynamic PET/CT with arterial blood. The hepatobiliary excretion of ^{64}Cu is slower than e.g. bile acids [33] but importantly, the properties of the ^{64}Cu isotope allows for long-term studies of copper metabolism in humans.

Conclusion

For intravenous administration, the gender-averaged effective dose was 62 ± 5 μSv/MBq with the liver being the most critical organ. For oral administration, significant residual radiotracer in the gastrointestinal tract resulted in high radiation doses to the intestines, particularly the right large intestine, leading to an effective dose of 113 ± 1 μSv/MBq. We found that both intravenous and oral administration of 50 MBq ^{64}Cu was sufficient for sequential studies in humans, yielding images of high quality up to 20 hours after administration with radiation doses approximately 3.1 mSv and 5.7 mSv, respectively. Moreover, the hepatic uptake from blood was comparable between the two administration forms when corrected for net intestinal absorption. Thus, ^{64}Cu PET/CT by intravenous and oral administration represent suitable methods for assessment of copper metabolism in humans, including the intestinal absorption, hepatic removal kinetics, and subsequent redistribution of copper.

Declarations

Acknowledgements: The authors would like to thank the participants for enrolling in this study as well as the staff from the Department of Nuclear Medicine and PET-Centre, Aarhus University Hospital, for experimental assistance.

Author contributions: *TS*, *SK*, *HV*, *PO*, *LG* and *OLM* conceived the study. *TS*, *SK* and *LG* performed the experimental procedures and *KF* and *KV* were in charge of the radiochemistry. *KK* analysed data, performed statistical analyses and wrote the first draft of the manuscript together with *TS*, *LG* and *OLM*. All authors contributed to, read, and approved the final manuscript.

Compliance with ethical standards: The study was approved by the Danish Medicines Agency (EudraCT no. 2016-001975-59) and the Central Denmark Region Committees on Health Research Ethics, conducted in accordance with the Helsinki II Declaration, and monitored by the Good Clinical Practice Unit (Aarhus University).

Funding: This study was supported by an unrestricted research grant from the Foundation of Manufacturer Vilhelm Pedersen and Wife.

Conflicts of interest: The authors declare that they have no conflicts of interest.

Consent for publication: All participants signed written informed consent for participation in the study and regarding publication of their data and images.

Availability of data and material: The datasets generated and analysed during the current study are available from the corresponding author on reasonable request.

References

1. Tapiero H, Townsend DM, Tew KD. Trace elements in human physiology and pathology. Copper Biomedicine pharmacotherapy = Biomedecine pharmacotherapie. 2003;57:386–98. doi:.

2. Gupta A, Lutsenko S. Human copper transporters: mechanism, role in human diseases and therapeutic potential. Future medicinal chemistry. 2009;1:1125–42. doi:.
3. Ala A, Walker AP, Ashkan K, Dooley JS, Schilsky ML. Wilson's disease. Lancet. 2007;369:397–408. doi:.
4. Avila-Rodriguez MA, Rios C, Carrasco-Hernandez J, Manrique-Arias JC, Martinez-Hernandez R, Garcia-Perez FO, et al. Biodistribution and radiation dosimetry of [(64)Cu]copper dichloride: first-in-human study in healthy volunteers. EJNMMI research. 2017;7:98. doi:.
5. Capasso E, Durzu S, Piras S, Zandieh S, Knoll P, Haug A, et al. Role of (64)CuCl 2 PET/CT in staging of prostate cancer. Annals of nuclear medicine. 2015;29:482–8. doi:.
6. Piccardo A, Paparo F, Puntoni M, Righi S, Bottoni G, Bacigalupo L, et al. (64)CuCl2 PET/CT in Prostate Cancer Relapse. Journal of nuclear medicine: official publication. Society of Nuclear Medicine. 2018;59:444–51. doi:.
7. Panichelli P, Villano C, Cistaro A, Bruno A, Barbato F, Piccardo A, et al. Imaging of Brain Tumors with Copper-64 Chloride: Early Experience and Results. Cancer Biother Radiopharm. 2016;31:159–67. doi:.
8. Wachsmann J, Peng F. Molecular imaging and therapy targeting copper metabolism in hepatocellular carcinoma. World journal of gastroenterology. 2016;22:221–31. doi:.
9. Peng F, Lu X, Janisse J, Muzik O, Shields AF. PET of human prostate cancer xenografts in mice with increased uptake of 64CuCl2. Journal of nuclear medicine: official publication. Society of Nuclear Medicine. 2006;47:1649–52.
10. McParland BJ. Nuclear medicine radiation dosimetry. Advanced theoretical principles. London: Springer; 2010. p. 568.
11. Munk OL, Bass L, Roelsgaard K, Bender D, Hansen SB, Keiding S. Liver kinetics of glucose analogs measured in pigs by PET: importance of dual-input blood sampling. Journal of nuclear medicine: official publication Society of Nuclear Medicine. 2001;42:795–801.
12. Holden JE, Doudet D, Endres CJ, Chan GL, Morrison KS, Vingerhoets FJ, et al. Graphical analysis of 6-fluoro-L-dopa trapping: effect of inhibition of catechol-O-methyltransferase. Journal of nuclear medicine: official publication Society of Nuclear Medicine. 1997;38:1568–74.
13. Logan J, Fowler JS, Volkow ND, Wolf AP, Dewey SL, Schlyer DJ, et al. Graphical analysis of reversible radioligand binding from time-activity measurements applied to [N-11C-methyl]-(-)-cocaine PET studies in human subjects. Journal of cerebral blood flow metabolism: official journal of the International Society of Cerebral Blood Flow Metabolism. 1990;10:740–7. doi:.
14. Stabin MG, Siegel JA. RADAR Dose Estimate Report: A Compendium of Radiopharmaceutical Dose Estimates Based on OLINDA/EXM Version 2.0. Journal of nuclear medicine: official publication. Society of Nuclear Medicine. 2018;59:154–60. doi:.
15. Basic anatomical and. physiological data for use in radiological protection: reference values. A report of age- and gender-related differences in the anatomical and physiological characteristics of reference individuals. ICRP Publication 89 Annals of the ICRP. 2002;32:5–265.

16. The 2007 Recommendations of the International Commission on Radiological Protection. ICRP publication 103. Ann ICRP. 2007;37:1–332. doi:.
17. Nyasae L, Bustos R, Braiterman L, Eipper B, Hubbard A. Dynamics of endogenous ATP7A (Menkes protein) in intestinal epithelial cells: copper-dependent redistribution between two intracellular sites. American journal of physiology Gastrointestinal liver physiology. 2007;292:G1181-94. doi:.
18. Winge DR. Normal physiology of copper metabolism. Seminars in liver disease. 1984;4:239–51. doi:.
19. Matte JJ, Girard CL, Guay F. Intestinal fate of dietary zinc and copper: Postprandial net fluxes of these trace elements in portal vein of pigs. Journal of trace elements in medicine biology: organ of the Society for Minerals Trace Elements (GMS). 2017;44:65–70. doi:.
20. Janssens AR, Van den Hamer CJ. Kinetics of 64Copper in primary biliary cirrhosis. Hepatology. 1982;2:822–7. doi:.
21. Cousins RJ. Absorption, transport, and hepatic metabolism of copper and zinc: special reference to metallothionein and ceruloplasmin. Physiological reviews. 1985;65:238–309. doi:.
22. Zhou B, Gitschier J. hCTR1: a human gene for copper uptake identified by complementation in yeast. Proc Natl Acad Sci USA. 1997;94:7481–6. doi:.
23. Turnlund JR, Keyes WR, Anderson HL, Acord LL. Copper absorption and retention in young men at three levels of dietary copper by use of the stable isotope 65Cu. Am J Clin Nutr. 1989;49:870–8. doi:.
24. 10.1093/ajcn/67.5.1054S
Wapnir RA. Copper absorption and bioavailability. The American journal of clinical nutrition. 1998;67:1054s-60 s. doi:.
25. Sternlieb I. Copper and the liver. Gastroenterology. 1980;78:1615–28.
26. Marceau N, Aspin N. Distribution of ceruloplasmin- ceruloplasmin-bound 67 Cu in the rat. Am J Physiol. 1972;222:106–10. doi:.
27. Alda JO, Garay R. Chloride (or bicarbonate)-dependent copper uptake through the anion exchanger in human red blood cells. Am J Physiol. 1990;259:C570-6. doi:.
28. Sternlieb I, Scheinberg IH. Radiocopper in diagnosing liver disease. Seminars in nuclear medicine. 1972;2:176–88.
29. Gunther K, Lossner V, Lossner J, Biesold D. The kinetics of copper uptake by the liver in Wilson's disease studied by a whole-body counter and a double labelling technique. European neurology. 1975;13:385–94. doi:.
30. Harvey LJ, Dainty JR, Hollands WJ, Bull VJ, Beattie JH, Venelinov TI, et al. Use of mathematical modeling to study copper metabolism in humans. Am J Clin Nutr. 2005;81:807–13. doi:.
31. Czlonkowska A, Rodo M, Wierzchowska-Ciok A, Smolinski L, Litwin T. Accuracy of the radioactive copper incorporation test in the diagnosis of Wilson disease. Liver international: official journal of the International Association for the Study of the Liver. 2018;38:1860–6. doi:.
32. Peng F, Lutsenko S, Sun X, Muzik O. Imaging copper metabolism imbalance in Atp7b (-/-) knockout mouse model of Wilson's disease with PET-CT and orally administered 64CuCl2. Molecular imaging

and biology: MIB : the official publication of the Academy of Molecular Imaging. 2012;14:600–7. doi:.

33. Ørntoft NW, Munk OL, Frisch K, Ott P, Keiding S, Sørensen M. Hepatobiliary transport kinetics of the conjugated bile acid tracer 11C-CSar quantified in healthy humans and patients by positron emission tomography. Journal of hepatology. 2017;67:321–7. doi:.

Figures

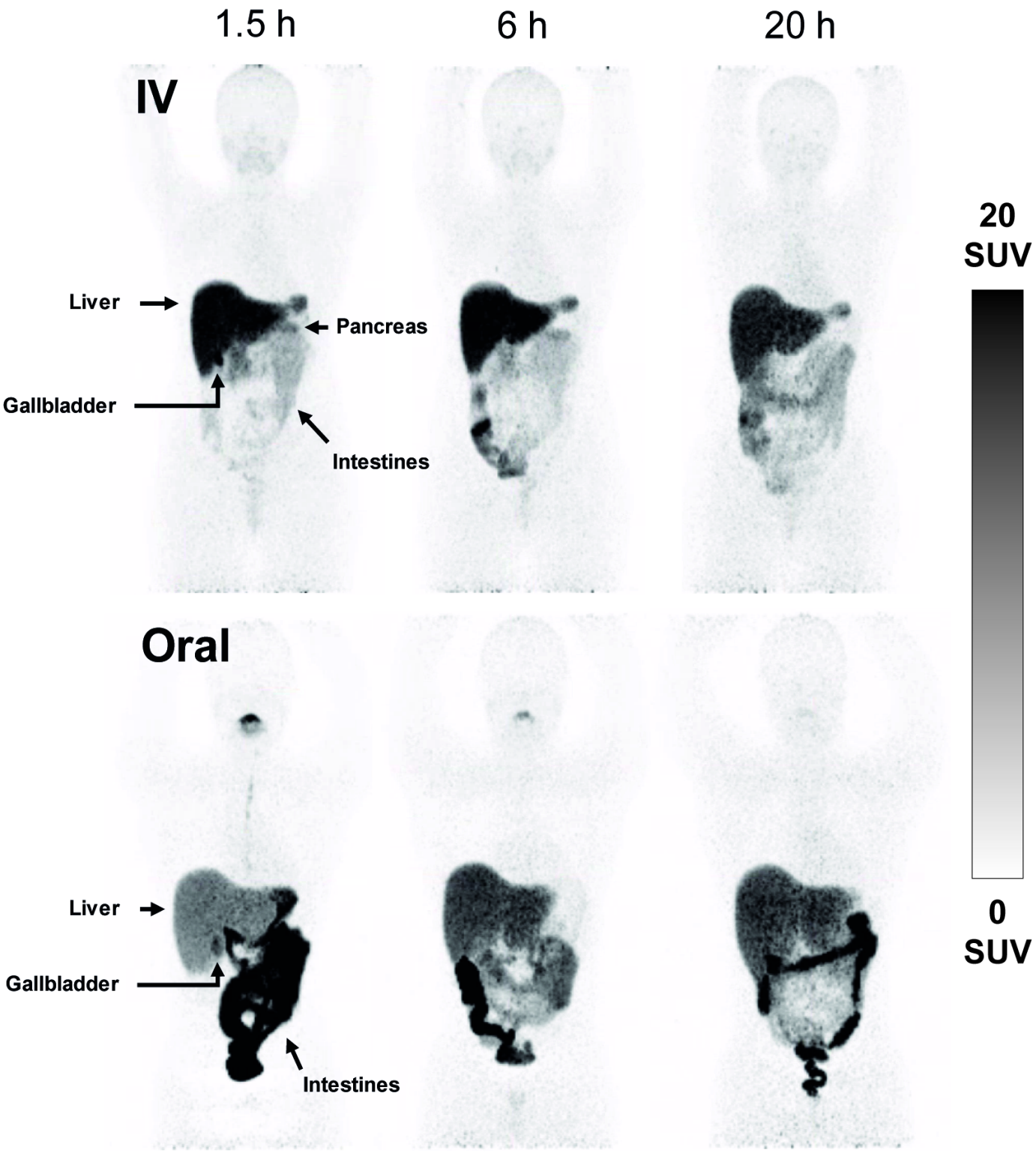

Figure 1

Whole-body PET images (maximum intensity projection) showing the biodistribution of 64Cu after intravenous (upper panels) and oral (lower panels) administration in two healthy individuals (IV4 and O2) PET imaging was performed 1.5, 6, and 20 h after administration. Arrows identify most visible source organs.

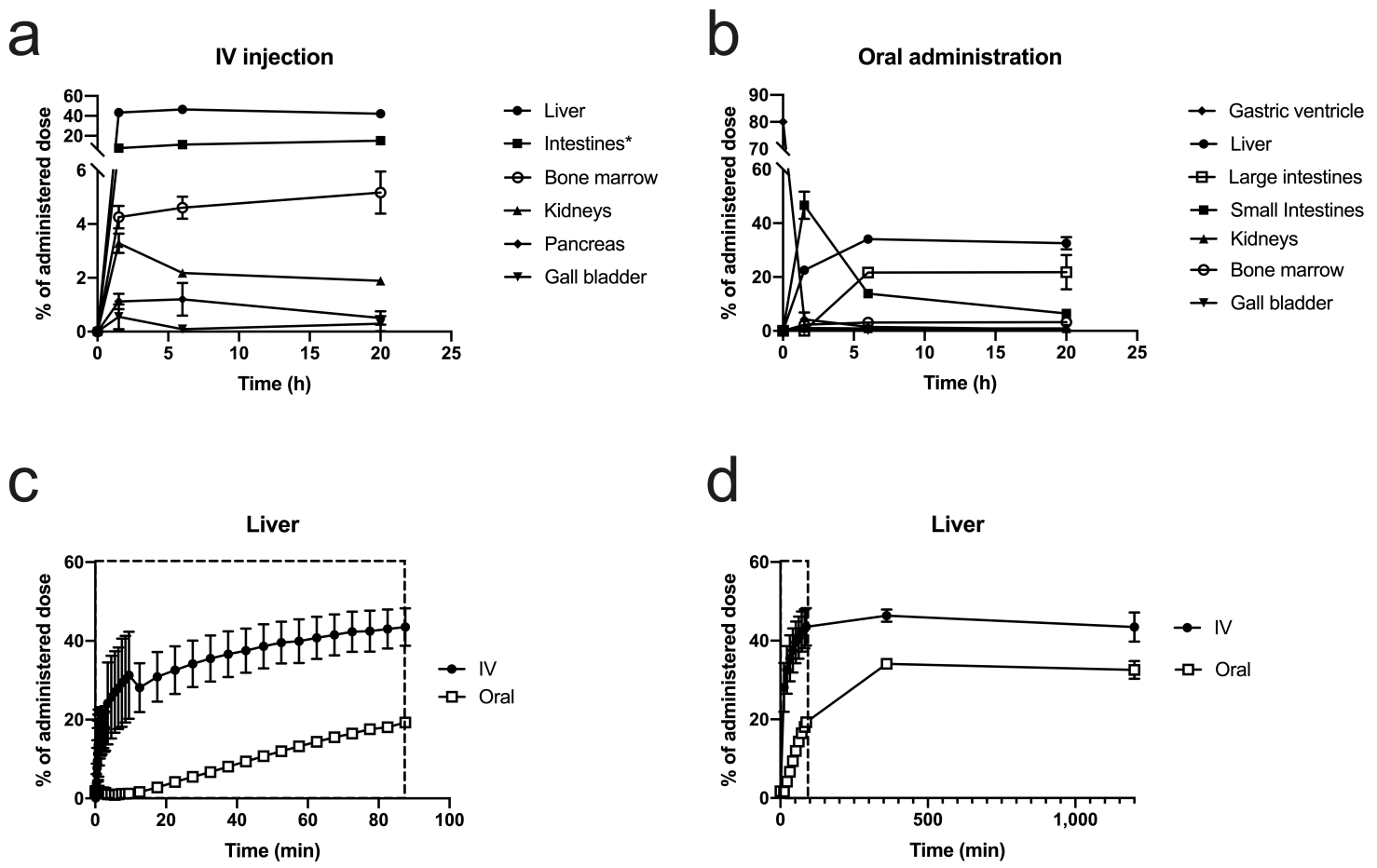

Figure 2

Time courses of %AD in source organs following intravenous (IV) and oral administration of 64Cu Upper panels show the biodistribution of 64Cu after IV (A) and oral (B) administration. Lower panels show %AD in liver tissue during the initial dynamic PET/CT scan (C; 90 min) and including static whole-body PET scans from the entire study period (D; 20 h); closed circles show the time course after IV administration, open circles after oral administration. All values are given as group means ± SD. *Summation of small and large intestine.

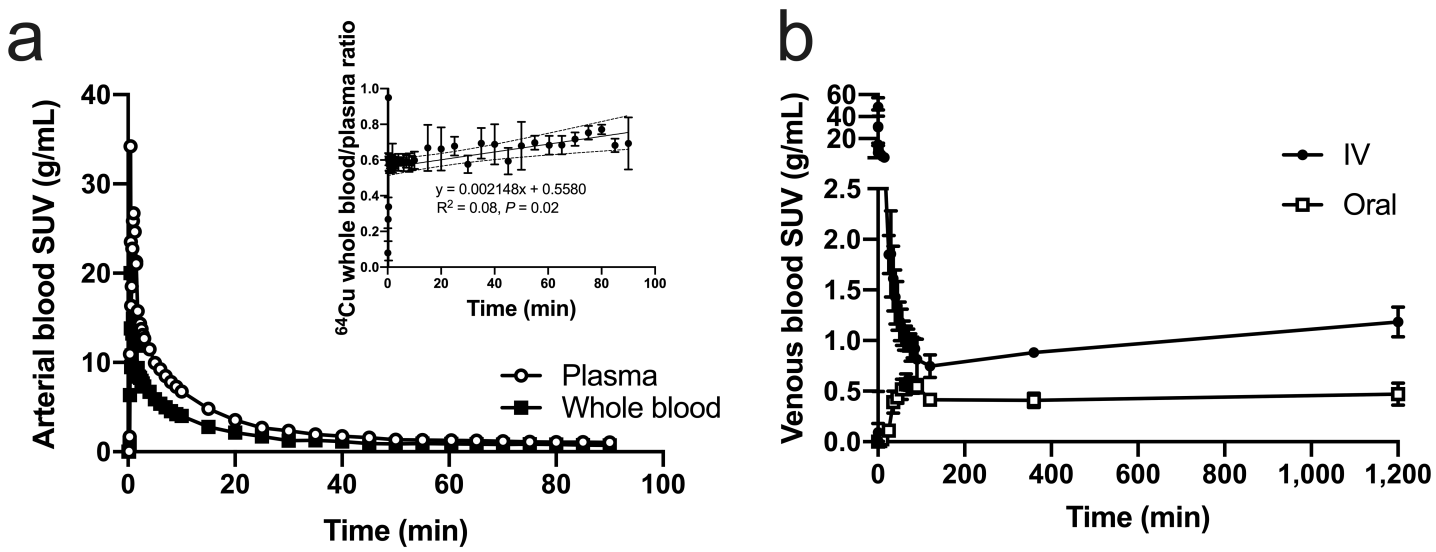

Figure 3

Time courses of the concentration of 64Cu in blood following administration intravenous (IV) and oral administration. Panel A shows whole blood (closed circles) and plasma (open circles) SUV in arterial blood following the initial 90 min after IV administration of 64Cu (n = 3; for clarity, no error bars are displayed); displayed as insert is the ratio between radioactivity concentration in whole blood and plasma. Panel B shows whole blood SUV in venous blood following IV and oral administration of 64Cu (n = 4 and n = 2, respectively). Values are given as group means ± SD.

Supplementary Files

This is a list of supplementary files associated with this preprint. Click to download.

- 64CuSUPPLEMENTAL.pdf